

การวิเคราะห์การสั่นไหวอิสระของคานประกอบระดับนาโนขั้นสูง

Free vibration analysis of advanced nanocomposite beams

ธนธรณ์ วรรณจิรวีไล¹ และ ศ. ดร. จรุง รุ่งอมรรัตน์²

^{1,2} ภาควิชาวิศวกรรมโยธา คณะวิศวกรรมศาสตร์ จุฬาลงกรณ์มหาวิทยาลัย จ. กรุงเทพฯ

Abstract

This senior project focuses on the investigation of free vibration and fundamental frequencies of functionally graded metal-ceramic nanocomposite beams with GPLs dispersed inside. Matrix materials gradation and GPLs distribution are varied in thickness dimension. Fundamental frequency is calculated by Isogeometric Analysis method based on Timoshenko beam theory and Hamilton's principle by finding the least eigenvalue from the equation system. The approximated answer of dimensionless fundamental frequency will be compared with results from Ritz method to represent the accuracy of the calculation.

Keywords: Isogeometric analysis, functionally graded material, nanocomposite beams

1. Introduction

1.1 Motivation and Significance

The study and development of advanced materials with more complexity have become popular recently, especially functionally graded materials and nanofibers reinforcement which leads to significantly improve the material's performance.

Metal is one of the materials for FGMs since it has a lighter weight compared to concrete and a higher stiffness-to-weight ratio. There are many studies about optimizing steel such as porous metals and metallic foam [1], [2].

Many studies indicated that FGMs fabrication allows us to determine and control material properties. Even with limitations due to real-life fabrication processes, FGMs properties can be properly determined and controlled in various methods [3], [4], [5].

Ideas of using metals and ceramics as FGMs can be enhanced with nanofibers reinforcement which will greatly increase the material's modulus and strength while also reducing the material's density.

1.2 Literature review

There are many studies about FGMs using various methods and theories which include free vibration analysis that is related to structural application. Shafiei et al. [6] studied nonlinear vibration of porous and imperfect FG microbeams. Using modified couple stress and Euler–Bernoulli theories as beams model, Hamilton's principle with Von-Kármán's nonlinear strain considered was used to obtain differential governing equations.

Chen et al. [7] studied free and forced vibration of FG beams by using a framework of Timoshenko beam theory including the effect of transverse shear strain then Lagrange equation method and Ritz trial functions are used to derive and obtain natural frequencies. The mentioned studies can be applied to FGMs which use two different materials instead of porosity.

Studies about nanofibers materials such as Carbon nanotubes (CNTs) and Graphene platelets (GPLs) are published with various analysis. Rafiee et al. [8] studied two nanofillers CNTs and GPLs to compare both properties. The experiment

results showed that GPLs provide better enhancement for mechanical properties compared to CNTs at same weight fraction.

Kittipornchai et al. [9] studied free vibration and elastic buckling FG porous beams reinforced by GPLs by dividing beams section into many layers while each layer has different pores and GPLs contents. Halpin-Tsai micromechanics model was used to obtain elastic modulus of the nanocomposite, while density and Poisson's ratio are calculated from rule of mixture. Governing equations are derived from Timoshenko beam theory while considering axial deformation and results are obtained from Ritz method with polynomial basis functions.

1.3 Objective

To investigate the behavior of beams made from FGMs with GPLs reinforcement under free vibration.

1.4 Scope of work

This project focuses on 1 span beam with simple supports under linear free vibration. The beam's matrix was made from FGMs varying in the z-axis and GPLs dispersion varying in the z-axis.

1.5 Methodology

This project will use same the workflow as Kitipornchai et al. [9] but with a different matrix which will be graded by using two materials together instead of grading by the porosity of the beams.

The beam's matrix material's effective properties can be obtained by using rule of mixture to calculate matrix properties, which will be used to calculate the composite effective modulus by using Halpin-Tsai micromechanics model while density and Poisson's ratio were calculated by rule of mixture [8], [10], [11].

Timoshenko beam theory was used to describe beam behavior with shear deformation considered and Hamilton's Principle was used to determine eigenvalue of the system which describes behavior of the beam.

After obtained governed the equation we will use Isogeometric Analysis (IGA) to analyze the beam by using B-spline as basis function which has piecewise properties since IGA can be used to solve problems with more complexity while using less resource and gives more accurate results compared to classic finite element analysis.

2. Problem formulation

2.1 Effective properties

To calculate elastic modulus of nanocomposite materials we use Halpin-Tsai micromechanics model [8], [10], [11].

$$E_c = \frac{3}{8} \frac{1 + \xi_{11} \eta_{11} V_{GPL}}{1 - \eta_{11} V_{GPL}} E_m + \frac{5}{8} \frac{1 + \xi_{22} \eta_{22} V_{GPL}}{1 - \eta_{22} V_{GPL}} E_m \quad (1)$$

$$\eta_{11} = \frac{(E_{GPL}/E_m) - 1}{(E_{GPL}/E_m) + \xi_{11}} \quad (2)$$

$$\eta_{22} = \frac{(E_{GPL}/E_m) - 1}{(E_{GPL}/E_m) + \xi_{22}} \quad (3)$$

$$\xi_{11} = 2 \left(\frac{l}{t} \right) \quad (4)$$

$$\xi_{22} = 2 \left(\frac{w}{t} \right) \quad (5)$$

Where:

E_c = effective elastic modulus of nanocomposite material

E_m = elastic modulus of matrix

E_{GPL} = elastic modulus of GPLs

V_{GPL} = Volume fractions of GPLs

ξ_{11} = Shape size parameter along longitudinal direction of GPLs

ξ_{22} = Shape size parameter transverse direction of GPLs

l, w, t = average length, width, thickness of GPLs

Elastic modulus, Poisson's ratio and mass density of matrix can be calculated by rule of mixture.

$$E_m = E_{metal} V_{metal} + E_{ceramic} V_{ceramic} \quad (6)$$

$$\nu_m = \nu_{metal} V_{metal} + \nu_{ceramic} V_{ceramic} \quad (7)$$

$$\rho_m = \rho_{metal} V_{metal} + \rho_{ceramic} V_{ceramic} \quad (8)$$

Where:

ν_m = Poisson's ratio of matrix

ρ_m = density of matrix

Using rule of mixture, Poisson's ratio and mass density of nanocomposite material can be described as:

$$\nu_c = \nu_m V_m + \nu_{GPL} V_{GPL} \quad (9)$$

$$\rho_c = \rho_m V_m + \rho_{GPL} V_{GPL} \quad (10)$$

Where:

V_m = Volume fractions of matrix ($V_m = 1 - V_{GPL}$)

ν_c = Poisson's ratio of nanocomposite material

ρ_c = Density of nanocomposite material

Shear modulus can be determined as:

$$G_c = \frac{E_c}{2(1 + \nu_c)} \quad (11)$$

Where:

E_c = Effective elastic modulus of nanocomposite material

G_c = Effective shear modulus of nanocomposite material

2.2 GPLs dispersion and Matrix distribution patterns

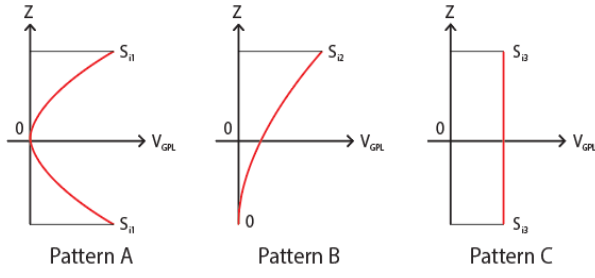


Fig 1. GPLs dispersion patterns

Three GPLs dispersion were used to vary volume fraction of GPLs along z-axis which can be written as:

$$V_{GPL} = S_{i1} \left[1 - \cos\left(\frac{\pi z}{h}\right) \right] \quad \text{For Pattern A} \quad (12a)$$

$$V_{GPL} = S_{i2} \left[1 - \cos\left(\frac{\pi z}{2h} + \frac{\pi}{4}\right) \right] \quad \text{For Pattern B} \quad (12b)$$

$$V_{GPL} = S_{i3} \quad \text{For Pattern C} \quad (12c)$$

Where:

$$V_{GPL} = \text{Volume fractions of GPLs where } -\frac{h}{2} \leq z \leq \frac{h}{2}$$

S_{ij} = Peak value of V_{GPL} for nanocomposite with GPLs dispersion pattern j (A, B, C) and matrix grading pattern i (1, 2, 3)

which can be determined by equations below:

$$S_{i1} = V_{GPL,t} \times h / \left[\int_{-h/2}^{h/2} 1 - \cos\left(\frac{\pi z}{h}\right) dz \right] \quad (13a)$$

$$S_{i2} = V_{GPL,t} \times h / \left[\int_{-h/2}^{h/2} 1 - \cos\left(\frac{\pi z}{2h} + \frac{\pi}{4}\right) dz \right] \quad (13b)$$

$$S_{i3} = V_{GPL,t} \quad (13c)$$

Where:

$V_{GPL,t}$ = Total volume of fraction GPLs in nanocomposite beams which can be obtained from desired weight fraction of GPLs in equation below:

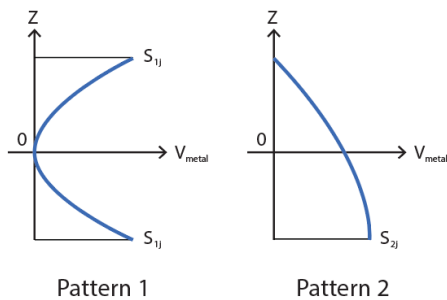
$$V_{GPL,t} = \frac{\text{Volume}_{GPL}}{\text{Volume}_{total}} = \frac{\frac{W_{GPL} \rho_{GPL}}{W_{GPL} + \frac{(1-W_{GPL})}{\rho_m}}}{\rho_{GPL} + \frac{(1-W_{GPL})}{\rho_m}} \quad (14)$$

Where:

W_{GPL} = Weight fraction of GPLs

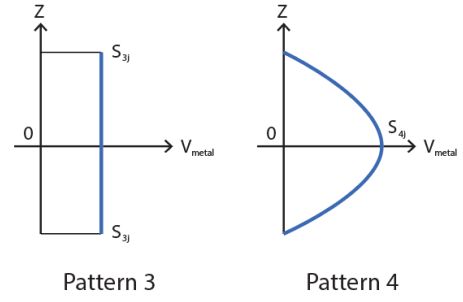
ρ_{GPL} = Density of GPLs

ρ_m = Density of matrix



Pattern 1

Pattern 2



Pattern 3

Pattern 4

Fig 2. GPLs dispersion patterns

Three matrix grading patterns were used by varying volume fraction of metal along z-axis to change elastic modulus which can be written as:

$$V_{metal} = S_{1j} \left(\frac{2z}{h}\right)^2 \quad \text{For Pattern 1} \quad (15a)$$

$$V_{metal} = S_{2j} \left[1 - \left(\frac{z}{h} + 0.5\right)^2 \right] \quad \text{For Pattern 2} \quad (15b)$$

$$V_{metal} = V_{metal,t} \quad \text{For Pattern 3} \quad (15c)$$

$$V_{metal} = S_{4j} \left[1 - \left(\frac{2z}{h}\right)^2 \right] \quad \text{For Pattern 4} \quad (15d)$$

Where:

$$S_{1j} = V_{metal,t} \times h / \left[\int_{-h/2}^{h/2} \left(\frac{2z}{h}\right)^2 dz \right]$$

$$S_{2j} = V_{metal,t} \times h / \left[\int_{-h/2}^{h/2} 1 - \left(\frac{z}{h} + 0.5\right)^2 dz \right]$$

$$S_{4j} = V_{metal,t} \times h / \left[\int_{-h/2}^{h/2} 1 - \left(\frac{2z}{h}\right)^2 dz \right]$$

$V_{metal,t}$ = Given total volume fraction of metal

3. Solution Techniques

3.1 Formulation

Using Timoshenko beam theory to describe beam's deformation which considered rotational of the section of the beam.

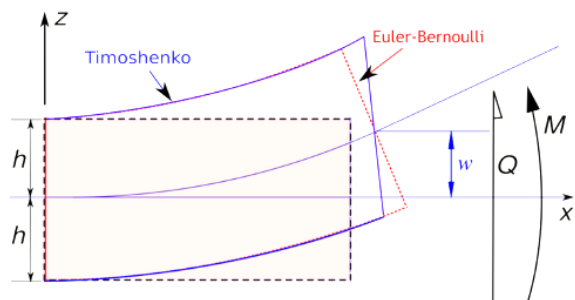


Fig 3. Timoshenko beam theory model

Displacement along x axis and z axis are defined as:

$$u_x = u_0 + z\phi_x \quad (16)$$

$$w_z = w_0 \quad (17)$$

Where:

u_0 = Axial displacement

w_0 = Transverse displacement at mid-plane ($z = 0$)

ϕ_x = Transverse normal rotation of z-axis

From fig 3. axial and transverse can be determined as:

$$\epsilon_{xx} = \frac{\partial u_0}{\partial x} + z \frac{\partial \phi_x}{\partial x} \quad (18)$$

$$\gamma_{xz} = \frac{\partial w_0}{\partial x} + \phi_x \quad (19)$$

Using linear stress-strain constitutive law, normal and

transverse can be determined as:

$$\sigma_{xx} = \frac{E(z)}{1-\nu(z)^2} \epsilon_{xx} = Q_{11}(z) \epsilon_{xx} \quad (20)$$

$$\sigma_{xz} = G(z) \gamma_{xz} = Q_{55}(z) \gamma_{xz} \quad (21)$$

Strain energy of the beam can be defined as:

$$U = \frac{1}{2} \int_0^L \int_{-h/2}^{h/2} (\sigma_{xx} \epsilon_{xx} + \sigma_{xz} \gamma_{xz}) dz dx \quad (22)$$

Substituting equations (18) – (21) into equation (22)

$$U = \frac{1}{2} \int_0^L \left[A_{11} \left(\frac{\partial u_0}{\partial x} \right)^2 + 2B_{11} \left(\frac{\partial u_0}{\partial x} \right) \left(\frac{\partial \phi_x}{\partial x} \right) + D_{11} \left(\frac{\partial \phi_x}{\partial x} \right)^2 + A_{55} \phi_x^2 + 2A_{55} \phi_x \left(\frac{\partial w_0}{\partial x} \right) + A_{55} \left(\frac{\partial w_0}{\partial x} \right)^2 \right] dx \quad (23)$$

Where:

$$\{A_{11}, B_{11}, D_{11}\} = \int_{-h/2}^{h/2} Q_{11}(z) \{1, z, z^2\} dz \quad (24)$$

$$A_{55} = \int_{-h/2}^{h/2} k Q_{55}(z) dz \quad (25)$$

$k = 5/6$ = Shear correction factor of the beam's section

Since there is no external force, external work W_e is equal to

0, then kinetic energy can be defined as:

$$T = \frac{1}{2} \int_0^L \left[I_0 \left(\frac{\partial u_0}{\partial t} \right)^2 + 2I_1 \left(\frac{\partial u_0}{\partial t} \right) \left(\frac{\partial \phi_x}{\partial t} \right) + I_2 \left(\frac{\partial \phi_x}{\partial t} \right)^2 + I_0 \left(\frac{\partial w_0}{\partial t} \right)^2 \right] dx \quad (26)$$

Where:

$$\{I_0, I_1, I_2\} = \int_{-h/2}^{h/2} \rho(z) \{1, z, z^2\} dz \quad (27)$$

Symbols for ease of display are defined as:

$$\{u'_0, w'_0, \phi'_x\} = \left\{ \frac{\partial u_0(x,t)}{\partial x}, \frac{\partial w_0(x,t)}{\partial x}, \frac{\partial \phi_x(x,t)}{\partial x} \right\} \quad (28)$$

$$\{\dot{u}_0, \dot{w}_0, \dot{\phi}_x\} = \left\{ \frac{\partial u_0(x,t)}{\partial t}, \frac{\partial w_0(x,t)}{\partial t}, \frac{\partial \phi_x(x,t)}{\partial t} \right\} \quad (29)$$

Using Hamilton's principle to create weak form of the

equation.

$$\int_{t_1}^{t_2} \delta T - \delta U + \delta W_e dt = 0 \quad \forall (t_1, t_2) \quad (30)$$

Variation of kinetic energy δT and variation of strain energy

δU can be written as:

$$\delta T = \int_0^L \left[I_0 \dot{u}_0 \delta \dot{u}_0 + I_1 (\dot{u}_0 \delta \dot{\phi}_x + \dot{\phi}_x \delta \dot{u}_0) + I_2 \dot{\phi}_x \delta \dot{\phi}_x + I_0 \dot{w}_0 \delta \dot{w}_0 \right] dx \quad (31)$$

$$\delta U \int_0^L \left[A_{11} u'_0 \delta u'_0 + B_{11} (u'_0 \delta \phi'_x + \phi'_x \delta u'_0) + D_{11} \phi'_x \delta \phi'_x + A_{55} (w'_0 \delta w'_0 + w'_0 \delta \phi_x + \phi_x \delta w'_0 + \phi_x \delta \phi_x) \right] dx \quad (32)$$

Substituting equations (31) – (32) into equation (30) and using integration by parts.

$$\int_0^L \left[\delta u'_0 (A_{11} u'_0 + B_{11} \phi'_x) + \delta \phi'_x (B_{11} u'_0 + D_{11} \phi'_x) + \delta \phi_x (A_{55} w'_0 + A_{55} \phi_x) + \delta w'_0 (A_{55} w'_0 + A_{55} \phi_x) \right] dx + \int_0^L \left[\delta u_0 (I_0 \ddot{u}_0 + I_1 \ddot{\phi}_x) + \delta \phi_x (I_1 \ddot{u}_0 + I_2 \ddot{\phi}_x) + \delta w_0 I_0 \ddot{w}_0 \right] dx = 0 \quad \forall (\delta u_0, \delta w_0, \delta \phi_x) \quad (33)$$

Variables are normalized and defined.

$$u = \frac{u_0}{h}, w = \frac{w_0}{h}, \phi = \phi_x, \xi = \frac{x}{L}, \eta = \frac{z}{h}$$

$$\tau = t \sqrt{\frac{A^*}{I^* L^2}}, a_{11} = \frac{A_{11}}{A^*}, b_{11} = \frac{B_{11}}{A^* h}$$

$$d_{11} = \frac{D_{11}}{A^* h^2}, a_{55} = \frac{A_{55}}{A^*}$$

$$t_0 = \frac{I_0}{I^*}, t_1 = \frac{I_1}{I^* h}, t_2 = \frac{I_2}{I^* h^2}, \omega = \Omega L \sqrt{\frac{A^*}{I^*}} \quad (34)$$

Where:

A^*, I^* are A_{11}, I_0 of pure metal beam without GPLs.

ω is dimensionless natural frequency.

Symbols for ease of display are defined as:

$$\{u', w', \phi'\} = \left\{ \frac{\partial u(\xi, \tau)}{\partial \xi}, \frac{\partial w(\xi, \tau)}{\partial \xi}, \frac{\partial \phi(\xi, \tau)}{\partial \xi} \right\} \quad (35)$$

Substituting equations (34) into equation (35)

$$\{u'_0, w'_0, \phi'_x\} = \left\{ \frac{u'}{\eta}, \frac{w'}{\eta}, \frac{\phi'}{L} \right\} \quad (36)$$

Substituting equations (34) and (36) into equation (33)

$$\frac{A^*}{\eta^2} \int_0^1 \left[\delta u' (a_{11} u' + b_{11} \phi') + \delta \phi' (b_{11} u' + d_{11} \phi') \right] d\xi + \frac{A^*}{\eta} \int_0^1 \left[\delta \phi a_{55} w' + \delta w' a_{55} \phi \right] d\xi + A^* \int_0^1 \left[\delta \phi a_{55} \phi \right] d\xi + h^2 I^* \int_0^1 \left[\delta u (t_0 \ddot{u} + t_1 \ddot{\phi}) + \delta \phi (t_1 \ddot{u} + t_2 \ddot{\phi}) + \delta w t_0 \ddot{w} \right] d\xi = 0 \quad \forall (\delta u, \delta w, \delta \phi) \quad (37)$$

Define u, w, ϕ as periodic function below:

$$\{u(\xi, \tau), w(\xi, \tau), \phi(\xi, \tau)\} = \{u^*(\xi), w^*(\xi), \phi^*(\xi)\} e^{i\omega \tau} \quad (38)$$

$$\{\ddot{u}, \ddot{w}, \ddot{\phi}\} = -\omega^2 \frac{A^*}{I^* L^2} \{u^*(\xi), w^*(\xi), \phi^*(\xi)\} e^{i\omega \tau} \quad (39)$$

Substituting equations (39) into equation (37)

$$\begin{aligned}
& \int_0^1 \left[\begin{array}{c} \delta(u^*)'(a_{11}(u^*)' + b_{11}(\phi^*)') \\ \delta(\phi^*)'(b_{11}(u^*)' + d_{11}(\phi^*)') \\ + \delta(w^*)'a_{55}(w^*)' \end{array} \right] d\xi \\
& + \eta \int_0^1 [\delta\phi^* a_{55}(w^*)' + \delta(w^*)' a_{55}\phi] d\xi \\
& + \eta^2 \int_0^1 [\delta\phi^* a_{55}\phi^*] d\xi \\
& - \omega^2 \int_0^1 \left[\begin{array}{c} \delta u^*(l_0 u^* + l_1 \phi^*) \\ + \delta\phi^*(l_1 u^* + l_2 \phi^*) + \delta w^* l_0 w^* \end{array} \right] d\xi \\
& = 0 \quad \forall (\delta u^*, \delta w^*, \delta \phi^*) \quad (40)
\end{aligned}$$

3.2. Vibration analysis

Using Isogeometric Analysis method [12], B-splines basis functions are created to approximate trial functions u^*, w^*, ϕ^* and test functions $\delta u^*, \delta w^*, \delta \phi^*$ which are piecewise linear on ξ and can be defined as:

For basis function order 0

$$N_{i,0}(\xi) = \begin{cases} 1 & \text{if } \xi_i \leq \xi \leq \xi_{i+1} \\ 0 & \text{otherwise} \end{cases} \quad (41)$$

For basis function order 1 and higher

$$\begin{aligned}
N_{i,p}(\xi) &= \frac{\xi - \xi_i}{\xi_{i+p} - \xi_i} N_{i,p-1}(\xi) \\
&+ \frac{\xi_{i+p+1} - \xi}{\xi_{i+p+1} - \xi_{i+1}} N_{i+1,p-1}(\xi) \quad (42)
\end{aligned}$$

Where:

i = index of basis function,

p = polynomial order of basis function

n = number of basis functions used to create B-spline curve

ξ_j = j^{th} knot from knot vector $\{\xi_1, \xi_2, \xi_3, \dots, \xi_{n+p}, \xi_{n+p+1}\}$

Uniform knot vector is used where ξ_j can be described as:

$$\begin{aligned}
& 0 \quad j \in [1, p+1] \\
& \xi_j = \begin{cases} \frac{j-p-1}{n-p} & j \in [p+2, n] \\ 1 & j \in [n, n+p] \end{cases} \quad (43)
\end{aligned}$$

Trial functions and test functions can be written in basis form

as:

$$\begin{aligned}
& \begin{pmatrix} u^*(\xi) \\ w^*(\xi) \\ \phi^*(\xi) \end{pmatrix} = N \times \begin{pmatrix} a_u \\ a_w \\ a_\phi \end{pmatrix} \\
& \begin{pmatrix} (u^*)'(\xi) \\ (w^*)'(\xi) \\ (\phi^*)'(\xi) \end{pmatrix} = N' \times \begin{pmatrix} a_u \\ a_w \\ a_\phi \end{pmatrix} \quad (44)
\end{aligned}$$

$$\begin{pmatrix} \delta u^*(\xi) \\ \delta w^*(\xi) \\ \delta \phi^*(\xi) \end{pmatrix} = \begin{pmatrix} \beta_u^T \\ \beta_w^T \\ \beta_\phi^T \end{pmatrix} \times N^T$$

$$\begin{pmatrix} \delta(u^*)'(\xi) \\ \delta(w^*)'(\xi) \\ \delta(\phi^*)'(\xi) \end{pmatrix} = \begin{pmatrix} \beta_u^T \\ \beta_w^T \\ \beta_\phi^T \end{pmatrix} \times (N')^T \quad (45)$$

Where:

$a_u, a_w, a_\phi, \beta_u, \beta_w, \beta_\phi$ are $n \times 1$ coefficient column vector defined as:

$$a_u = \begin{pmatrix} a_{u1} \\ a_{u2} \\ \vdots \\ a_{u(n-1)} \\ a_{un} \end{pmatrix}, a_w = \begin{pmatrix} a_{w1} \\ a_{w2} \\ \vdots \\ a_{w(n-1)} \\ a_{wn} \end{pmatrix}, a_\phi = \begin{pmatrix} a_{\phi1} \\ a_{\phi2} \\ \vdots \\ a_{\phi(n-1)} \\ a_{\phi n} \end{pmatrix} \quad (46a)$$

$$\beta_u = \begin{pmatrix} \beta_{u1} \\ \beta_{u2} \\ \vdots \\ \beta_{u(n-1)} \\ \beta_{un} \end{pmatrix}, \beta_w = \begin{pmatrix} \beta_{w1} \\ \beta_{w2} \\ \vdots \\ \beta_{w(n-1)} \\ \beta_{wn} \end{pmatrix}, \beta_\phi = \begin{pmatrix} \beta_{\phi1} \\ \beta_{\phi2} \\ \vdots \\ \beta_{\phi(n-1)} \\ \beta_{\phi n} \end{pmatrix} \quad (46b)$$

N is row vector of basis function power P .

$$N = \{N_{1,p}(\xi), N_{2,p}(\xi), \dots, N_{n-1,p}(\xi), N_{n,p}(\xi)\} \quad (47a)$$

$$\begin{aligned}
N' &= \left\{ \frac{d}{d\xi} N_{1,p}(\xi), \frac{d}{d\xi} N_{2,p}(\xi), \dots \right. \\
&\left. , \frac{d}{d\xi} N_{n-1,p}(\xi), \frac{d}{d\xi} N_{n,p}(\xi) \right\} \quad (47b)
\end{aligned}$$

Substituting equations (44) and (45) into equation (40) results in governing equation for vibration analysis which can be written as: $(K - \omega^2 M)a = 0$

Where:

K, M are $3n \times 3n$ stiffness matrix and $a, 0$ are $3n \times 1$ coefficients column vector and zero column vectors respectively. The complete governing equation will be used to study free vibration analysis of FGMs nanocomposite beams with a program developed via software MATLAB R2023a which will be discussed in the next section.

4. Results and Discussion

4.1 Validation

Various power of basis functions and control points are tested to see if the program provides convergence results, then Numerical results were compared with approximate solutions done by Kitipornchai et al. by using GPLs pattern A, C-C support condition, Pure copper matrix

Material and GPLs properties are:

$$E_m = 130 \text{ GPa}, \nu_m = 0.34, \rho_m = 8,960 \text{ kg/m}^3$$

$$E_{GPL} = 1,010 \text{ GPa}, \nu_m = 0.186, \rho_m = 1062.5 \text{ kg/m}^3$$

$$l_{GPL} = 2.5 \text{ } \mu\text{m}, w_{GPL} = 1.5 \text{ } \mu\text{m}, t_{GPL} = 1.5 \text{ nm}$$

Table 1 Comparison of dimensionless fundamental frequency (GPL = 0 wt.%)

GPLs Weight Fraction	Control points	Fundamental Frequency		
		P = 2	P = 3	P = 5
0 wt.%				
	4	1.0395	0.9398	-
	6	0.3835	0.3227	0.3175
	10	0.3203	0.3167	0.3167
	16	0.3170	0.3167	0.3167
	24	0.3167	0.3167	0.3167
Kitipornchai et al. [9]	-	0.3167		

Table 2 Comparison of dimensionless fundamental frequency (GPL = 1 wt.%)

GPLs Weight Fraction	Control points	Fundamental Frequency		
		P = 2	P = 3	P = 5
1 wt.%				
	4	1.3472	1.2207	-
	6	0.5291	0.4578	0.4516
	10	0.4547	0.4505	0.4505
	16	0.4509	0.4505	0.4505
	24	0.4506	0.4505	0.4505
	34	0.4505	0.4505	0.4505
Kitipornchai et al. [9]	-	0.4505		

From the comparison above, we can conclude that the program tends to have more accuracy when increasing control points or power of basis functions in the program, while the results also converge toward reference answers. A higher power basis requires lower control points to be converged. The highlighted cells show the number of control points that results are consistent.

Another validation was made by comparing dimensionless fundamental frequency of FGM Al_2O_3/Al beams without GPLs reinforcement from Wattanakulpong et al. [13] which use power law distribution for the beam's matrix. (L/H = 20, P = 3, n = 24, Results were proved to be convergence)

Material and GPLs properties are:

$$E_{ceramic} = 380 \text{ GPa}, \nu_{ceramic} = 0.3, \rho_{ceramic} = 3,960 \text{ kg/m}^3$$

$$E_{metal} = 70 \text{ GPa}, \nu_{metal} = 0.3, \rho_{metal} = 2,702 \text{ kg/m}^3$$

Use matrix distribution pattern 2 (nonsymmetric, nonuniform, maximum metal volume fraction at bottom of beam section)

Table 3 Comparison of dimensionless fundamental frequency (x L/H) of FGMs

power	Owner	Ref.[5]	power	Owner	Ref.[5]
C-C			C-F		
Al	6.3398	6.459	Al	1.0103	1.015
5	8.2064	8.314	5	1.3105	1.307
2	8.6575	8.732	2	1.3792	1.372
1	9.5128	9.555	1	1.5153	1.504
0.5	10.5429	10.571	0.5	1.6808	1.663
0.2	11.5452	11.566	0.2	1.8425	1.816
Al_2O_3	12.4477	12.43	Al_2O_3	1.9886	1.953

From the table, we can see that the maximum difference between the program and reference result is 1.84% by using power law for matrix distribution. Most C-F support results have higher frequencies compared to reference while most C-C have lower frequencies. It is noticeable that C-C support beams have significantly higher frequency compared to C-F support beams.

4.2 Matrix distribution and GPLs dispersion patterns

After program validation, natural frequencies provided from C-C support beams with various GPLs dispersion and matrix distribution patterns are compared to determine which dispersion and distribution patterns result in the highest frequency. (L/H = 20, P = 3, n = 24, Results were proved to be convergence) Material and GPLs properties are:

Metal and ceramic use same properties from previous validation

$$V_{metal,t} = 0.3, W_{GPL} = 0.01$$

$$E_{GPL} = 1,010 \text{ GPa}, \nu_{GPL} = 0.186, \rho_{GPL} = 1062.5 \text{ kg/m}^3$$

$$l_{GPL} = 2.5 \mu m, w_{GPL} = 1.5 \mu m, t_{GPL} = 1.5 \text{ nm}$$

Table 4 dimensionless fundamentals frequencies from various matrix distribution and GPLs dispersion patterns (L/H = 20, P = 3, n = 24, Results were proved to be convergence)

Matrix Distribution Patterns	GPLs dispersion Patterns		
	A	B	C
1	0.5424	0.5223	0.5194
2	0.6048	0.5859	0.5896
3	0.6018	0.5883	0.5862
4	0.6295	0.6184	0.6166

The results show that for each matrix distribution pattern, GPLs dispersion pattern A (symmetric, nonuniform, maximum GPLs volume fraction at top and bottom of beam section) has the highest frequency. For each GPLs distribution pattern, matrix distribution pattern 4 (symmetric, nonuniform, maximum metal volume fraction at top and bottom of beam section) has the highest frequency. The combination that has the highest frequency is matrix distribution pattern 4 and GPLs dispersion pattern A

Using the same properties (GPLs dispersion pattern A, matrix distribution pattern 4, $V_{metal,t} = 0.3$) and altering the weight fraction of GPLs would affect the fundamental frequencies, which can be shown in the graph below:

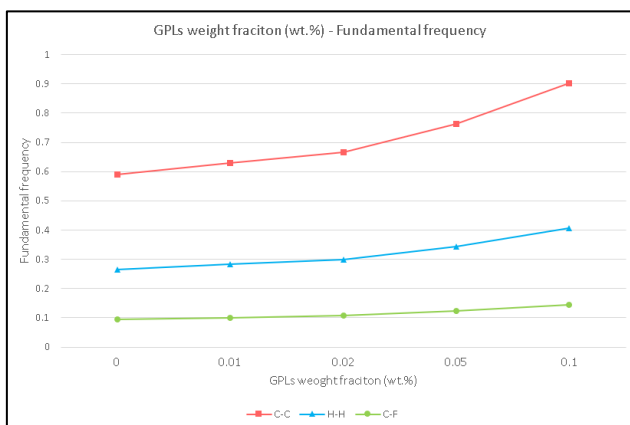


Fig 4. Relationship between fundamental frequency and GPLs weight fraction using different support conditions.

Using the same properties (GPLs dispersion pattern A, matrix distribution pattern 4, $W_{GPL} = 0.01$) and altering the total volume fraction metal would affect the fundamental frequencies, which can be shown in the graph below:

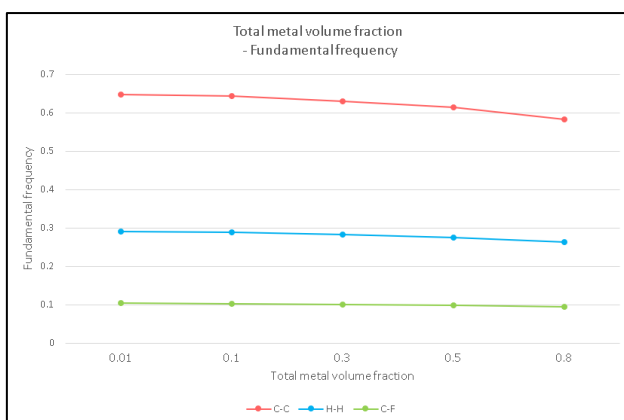


Fig 5. Relationship between fundamental frequency and total metal volume fraction using different support conditions.

5. Conclusion

This project studied and developed a program for calculating fundamental frequencies of FGMs nanocomposite beams using Isogeometric Analysis [12]. The process of calculation is based on work from Kitipornchai et al [9].

The displacements of the beam are determined by using Timoshenko beam theory, governing equation was created by using Hamilton's principle and fundamental frequencies were calculated from Isogeometric Analysis method via MATLAB.

The program was validated by comparing the answer with pure metal with GPLs beams from Kitipornchai et al. and proved to converge with various order of basis function and control points (as shown in Table 1 and Table 2) then compared with results of FGMs beams without GPLs from Wattanaskulpong et al [13].

After validation, the effects of different matrix distribution and GPLs dispersion was studied and found that symmetric matrix distribution with maximum metal volume fraction at midplane of the beam's section combined with symmetric GPLs dispersion pattern which has maximum GPLs fraction on top and bottom of the beam results in maximum frequency compared to other patterns combination (as shown in Table 4). Furthermore, the effects of GPLs weight fraction, Total metal volume fraction, beams slenderness, and power index were studied (as shown in fig 4, fig 5, and table 5).

In this project, the study and analysis only applied to Isogeometric Analysis of uniform B-splines basis function for 1D beams problems. While for future research Isogeometric Analysis of uniform B-splines basis function can be applied to more complex beam shape or properties.

References

- [1] [L.-P. Lefebvre, J. Banhart, D. Dunand, Porous metals and metallic foams: current status and recent developments, Adv. Eng. Mater. 10 \(2008\) 775–787.](#)
- [2] [B. Smith, S. Szyniszewski, J. Hajjar, B. Schafer, S. Arwade, Steel foam for structures: a review of applications, manufacturing and material properties, J. Constr. Steel Res. 71 \(2012\) 1–10.](#)
- [3] [A. Hassani, A. Habibolahzadeh, H. Bafti, Production of graded aluminum foams via powder space holder technique, Mater. Des. 40 \(2012\) 510–515.](#)

- [4] [S.-Y. He, Y. Zhang, G. Dai, J.-O. Jiang, Preparation of density-graded aluminum foam, Mater. Sci. Eng. A 618 \(2014\) 496–499.](#)
- [5] [Y. Hangai, K. Takahashi, T. Utsunomiya, S. Kitahara, O. Kuwazuru, N. Yoshikawa, Fabrication of functionally graded aluminum foam using aluminum alloy die castings by friction stir processing, Mater. Sci. Eng. A 534 \(2012\) 716–719.](#)
- [6] [N. Shafiei, A. Mousavi, M. Ghadiri, On size-dependent nonlinear vibration of porous and imperfect functionally graded tapered microbeams, Int. J. Eng. Sci. 106 \(2016\) 42–56.](#)
- [7] [D. Chen, J. Yang, S. Kitipornchai, Free and forced vibrations of shear deformable functionally graded porous beams, Int. J. Mech. Sci. 108 \(2016\) 14–22.](#)
- [8] [R., M. & Intelligence, Artificial & Wang, Zhou & Song, Huai-He & Yu, Zhong-Zhen & Koratkar, Nikhil. \(2009\). Enhanced Mechanical Properties of Nanocomposites at Low Graphene Content. ACS nano. 3. 3884-90. 10.1021/nn9010472.](#)
- [9] [S. Kitipornchai, D. Chen, J. Yang, Free vibration and elastic buckling of functionally graded porous beams reinforced by graphene platelets, Materials & Design \(2017\) 656-665.](#)
- [10] [M. Shokrieh, M. Esmkhani, Z. Shokrieh, Z. Zhao, Stiffness prediction of graphene nanoplatelet/epoxy nanocomposites by a combined molecular dynamics–micromechanics method, Comput. Mater. Sci. 92 \(2014\) 444–450.](#)
- [11] [J. Afdl, J. Kardos, The Halpin-Tsai equations: a review, Polym. Eng. Sci. 16 \(1976\) 344–352.](#)
- [12] J. Austin Cottrell, Thomas J. R. Hughes, Yuri Bazilevs. Isogeometric analysis: toward integration of CAD and FEA. John Wiley & Sons Ltd, The Atrium, Southern Gate, Chichester, West Sussex, PO19 8SQ, United Kingdom. (2009).
- [13] [N. Wattanasakulpong and V. Ungbhakorn. Free Vibration Analysis of Functionally Graded Beams with General Elastically End Constraints by DTM. World Journal of Mechanics, Vol. 2 No. 6, pp. 297-310. doi: 10.4236/wjm.2012.26036. \(2012\).](#)